Measurements of $\gamma p \to p\eta$ Differential Cross Sections and $\gamma p \to p\omega$ Differential Cross Sections and ρ^0, ρ^3 Using CLAS at Jefferson Lab: A Study of the Production Mechanisms

Tianqi Hu

Florida State University, Tallahassee, FL

Dissertation Defense

06/02/2022

Outline

Outline

Standard Model

- What are the most fundamental building blocks of our universe?
- How do these building blocks interact with each other and how do they form the diversity of our universe?

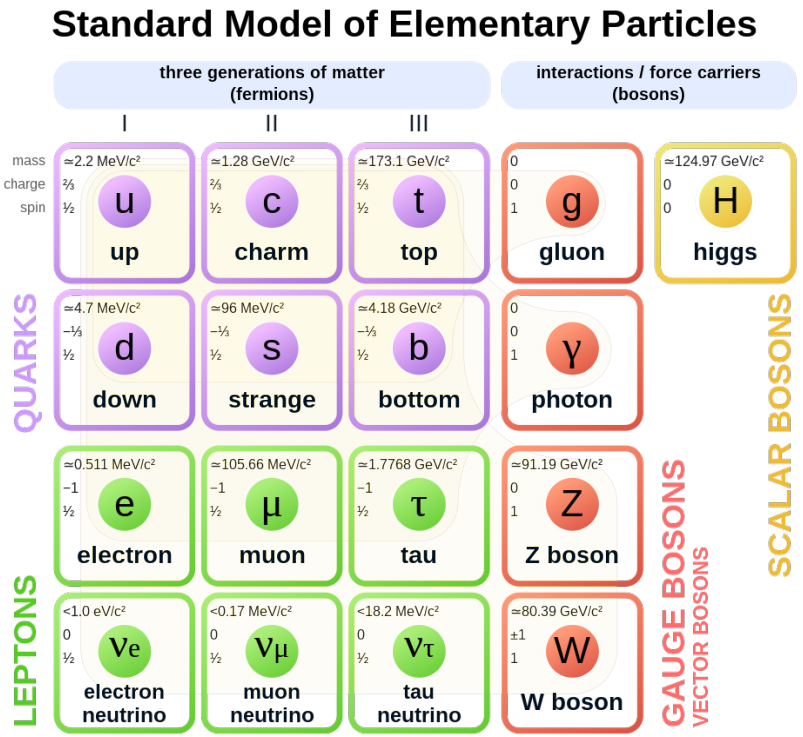

- Twelve elementary fermions.
- Four gauge bosons (vector bosons).
- The Higgs boson (scalar boson).

Pictures taken from `https://livescience.com` (left) and Wikipedia (right).

Quantum Chromodynamics (QCD)

- Quarks: the objects that experience the strong interaction.
- Gluons: the gauge bosons carrying the strong force.

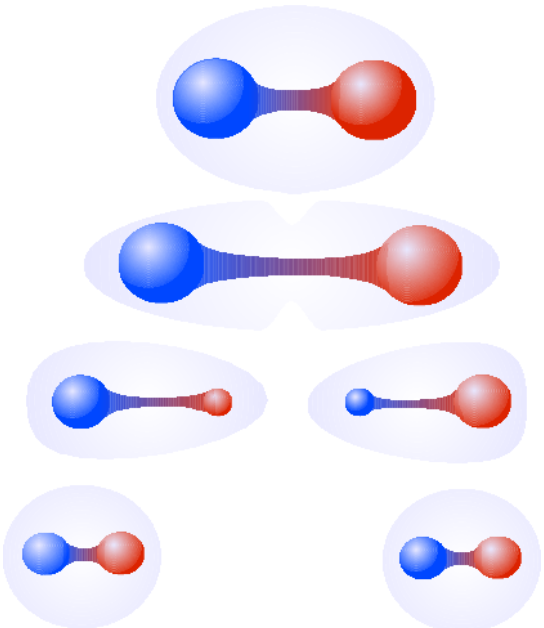

- Color confinement: Only particles with white color can be isolated.
- Asymptotic freedom: The strong coupling constant gets smaller at a smaller length scale (larger momentum transfer).

Q: What is the nature of color charge and what causes color confinement?

Pictures taken from `https://webific.ific.uv.es` (left) and `https://www.ectstar.eu` (right).

Hadrons & Quark Model

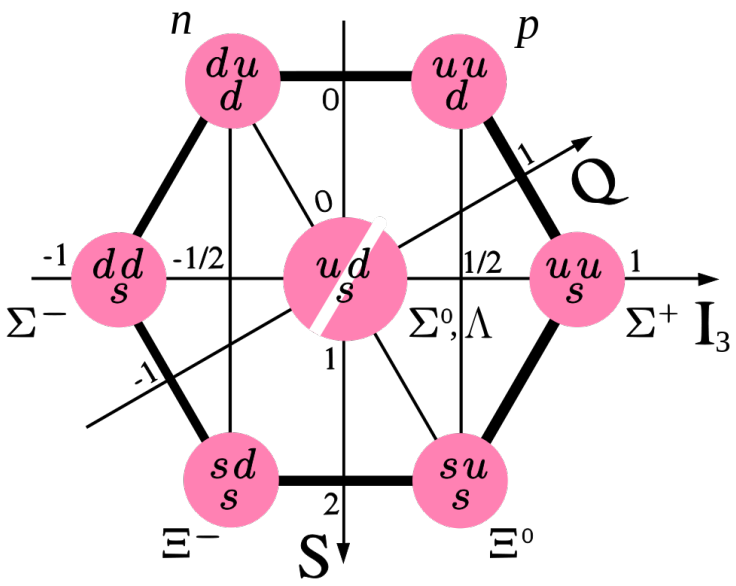

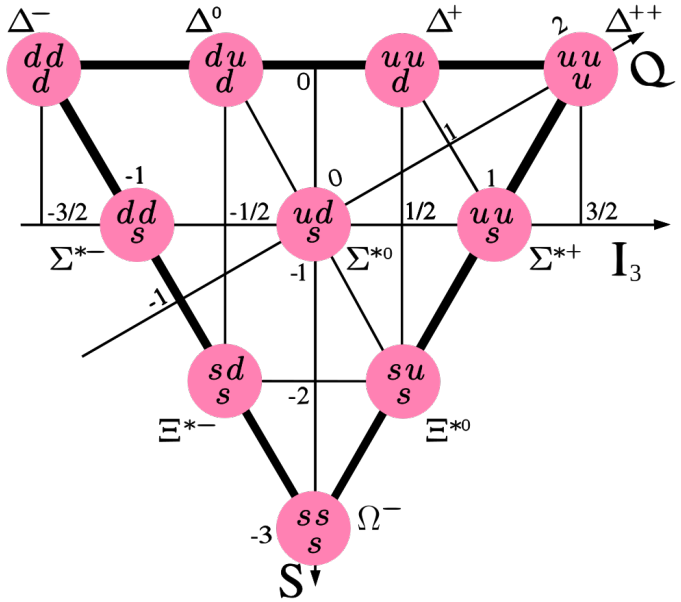

- Baryons: (qqq) fermions with half-integer spins
- Mesons: ($q\bar{q}$) bosons with integer spins

- Isospin symmetry was extended to the SU(3) flavor symmetry.
- SU(3) flavor symmetry $\Rightarrow$ spin-1/2 baryon octet and spin-3/2 decuplet.

Pictures taken from Wikipedia.

Baryon Resonance

- Baryon resonance: excited states of baryons.
- Providing a way to understand the degrees of freedom inside baryons.
- much more unstable (with a lifetime of $\sim 10^{-23} s$) than atoms

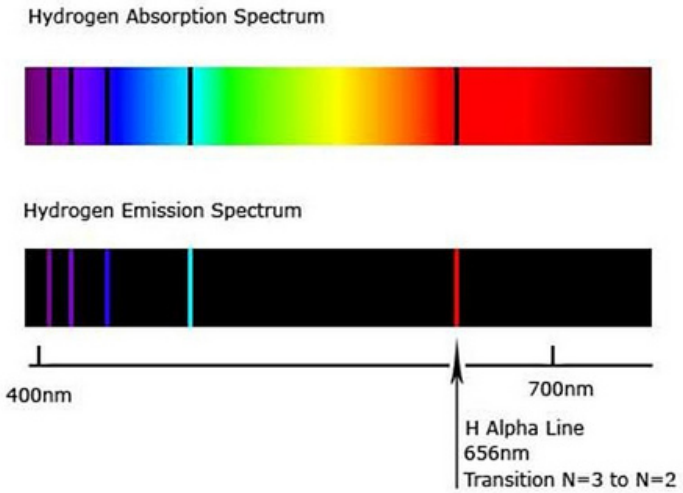

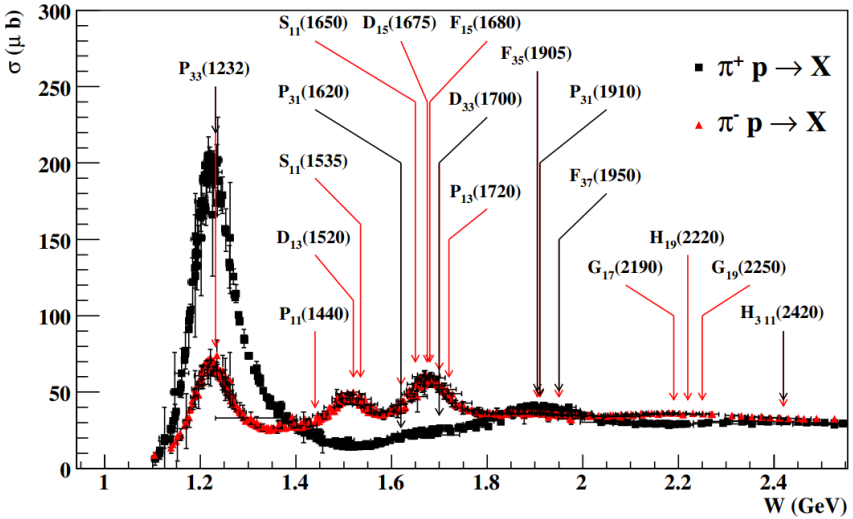

- Much broader line widths due to much shorter lifetimes.
- Techniques (partial wave analysis) required to disentangle the overlapped states.

Pictures taken from M. Williams, Ph.D. Thesis (2007) (left) and `www.khanacademy.org` (right).

Progress of η Meson Photoproduction Experiments

Reaction	W [GeV]	Observables	Collaboration
$\gamma p \to p\eta$	1.49-1.96	cross sections	A2
	1.55-2.80		CLAS
	1.51-2.55		CB-ELSA
	1.57-2.38		CBELSA/TAPS
	1.49-1.92		GRAAL
	1.97-2.32		LEPS
	2.36, 2.55		Daresbury
	2.90, 3.48		DESY
	2.90		MIT
	3.48-5.56		SLAC
	2.90-3.99		Cornell
	1.51-1.69	Σ observable	GRAAL
	1.49-1.91		CBELSA/TAPS
	1.70-2.10		CLAS
	1.49-1.87	T, F observables	A2
	1.45-2.15	E observable	CLAS
	1.49-1.87		A2
	1.48-2.40	T, E, P, H, G observables	CBELSA/TAPS
$\gamma n \to n\eta$	1.49-1.88	cross sections	A2
	1.50-2.18		CBELSA/TAPS
	1.59-2.07		CBELSA/TAPS
	1.49-1.87	E observable	A2

- η meson: $J^{PC} = 0^{-+}$ pseudoscalar meson.
- Important channel for extracting nucleon resonances.
- Few data above the nucleon resonance regime.
- Dominant decay channel $\eta \to \pi^+\pi^-\pi^0$.

Q: How are the η mesons produced in the pure scattering process above the resonance regime?

Reference can be found in the dissertation.

Progress of ω Meson Photoproduction Experiments

W [GeV]	Observables	Collaboration
2.62-2.87	cross sections	CLAS
1.71-1.87		A2
2.35-2.54	cross sections, ρ^0 SDMEs	SLAC, Daresbury
1.72-2.40		SAPHIR
1.7-2.8		CLAS
2.48, 3.14	ρ^0 SDMEs	LAMP2
1.74-2.36	cross sections, ρ^0, ρ^1, ρ^2 SDMEs	CBELSA/TAPS
1.72-2.02	Σ observable	CBELSA/TAPS
1.75-2.25	E, G observables	CBELSA/TAPS

- ω meson: $J^{PC} = 1^{--}$ vector meson, with the same J^{PC} quantum numbers as the photon.
- Spin-polarization can be revealed by measuring the spin density matrix elements (SDMEs) in its dominant decay channel $\omega \to \pi^+\pi^-\pi^0$.

Reference can be found in the dissertation.

Photoproduction Mechanism

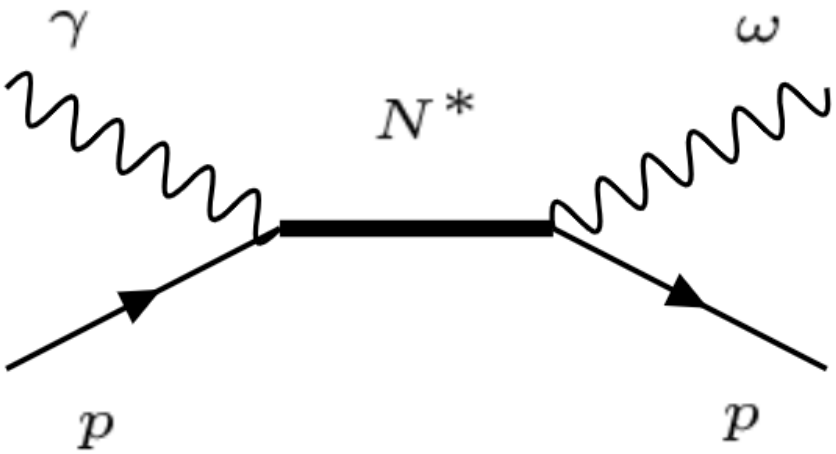

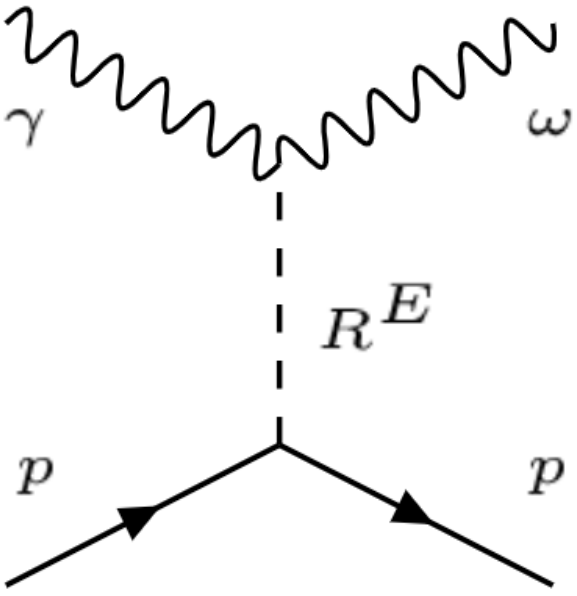

General picture of the photoproduction mechanism:
s-channel production through nucleon resonance decay (left) and *t*-channel production via exchange of Reggeons (right)

Outline

Jefferson Lab & CEBAF

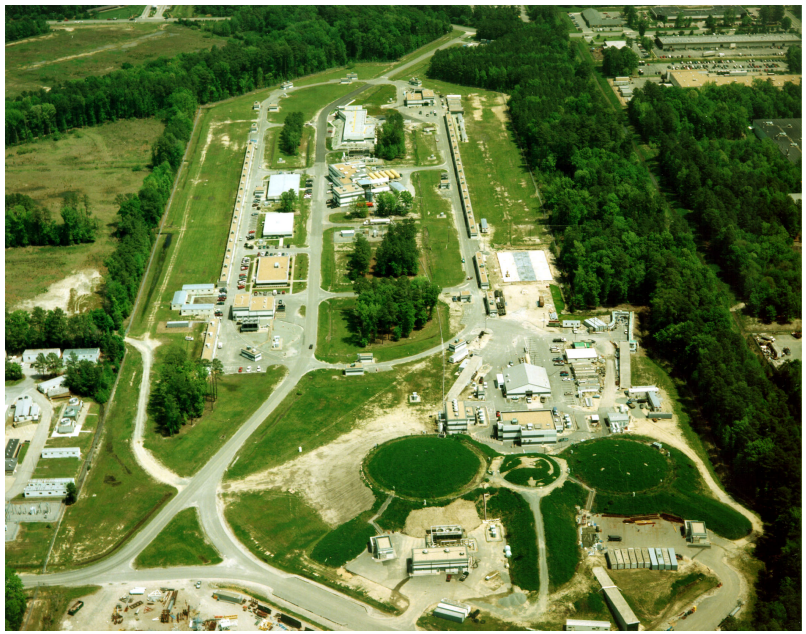

- Aerial view of Jefferson Lab@NewPort News.
- Accelerator: Continuous Electron Beam Accelerator Facility (CEBAF).
- CLAS Experiments taken in Hall B.

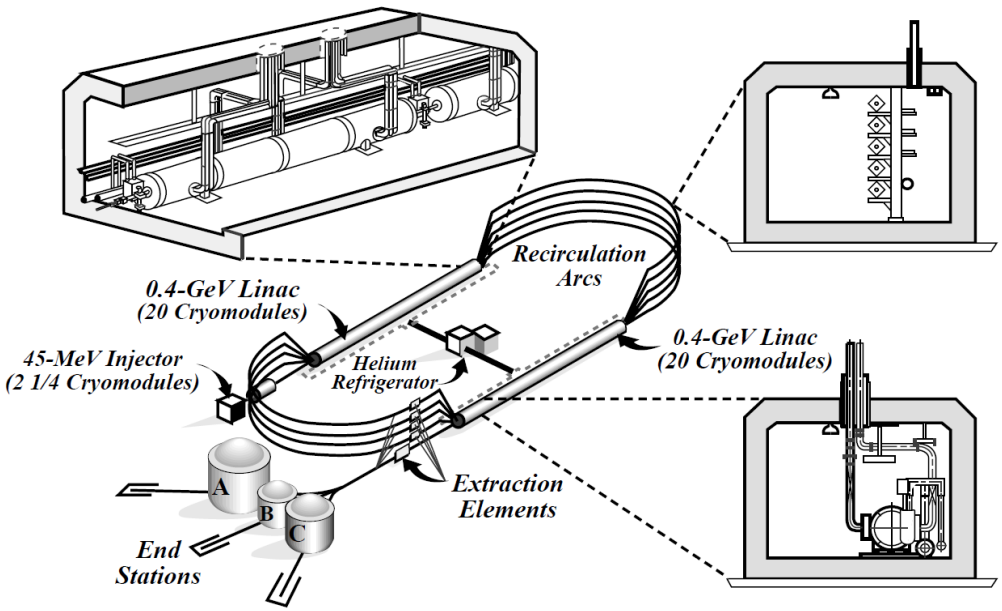

- Two linear accelerators (Linac) connected by two recirculation arcs.
- Linearly-polarized electrons $E_{e^-} = 5.715$ GeV (CLAS-g12), producing bremsstrahlung photons up to $E_\gamma = 5.45$ GeV.

Pictures taken from https://www.flickr.com/photos/jeffersonlab/.

The CLAS Spectrometer

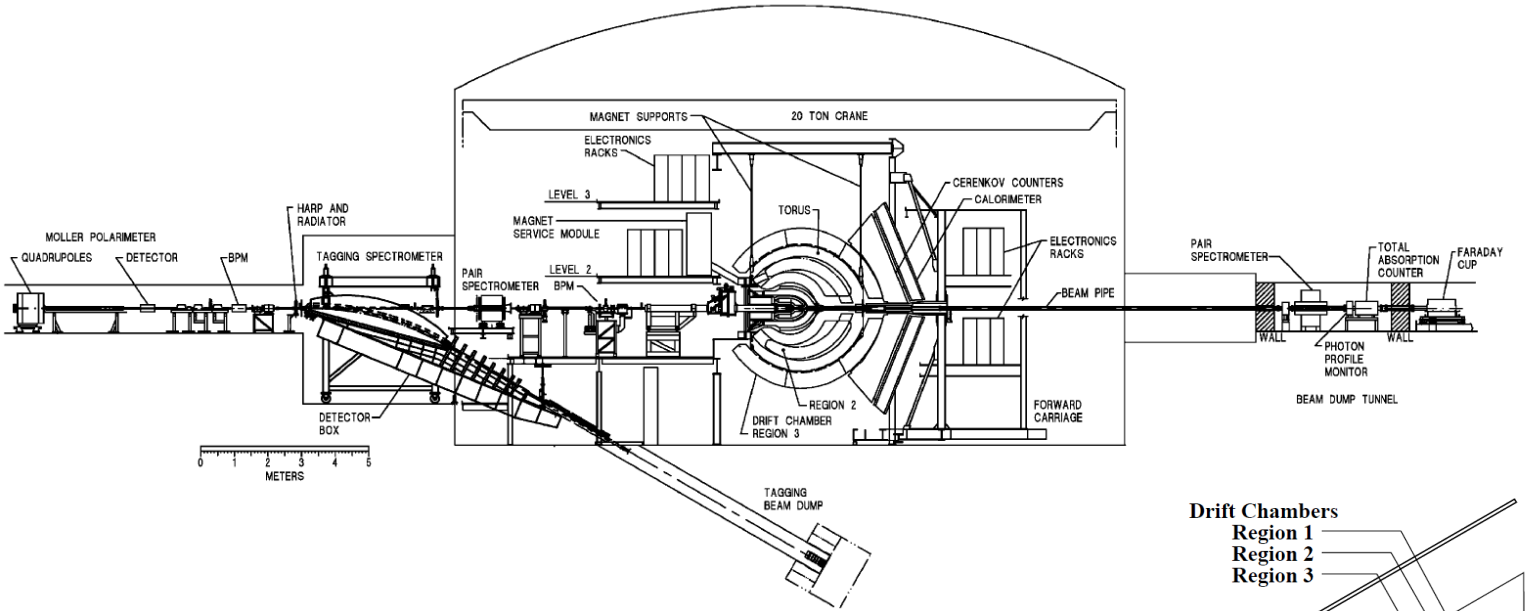

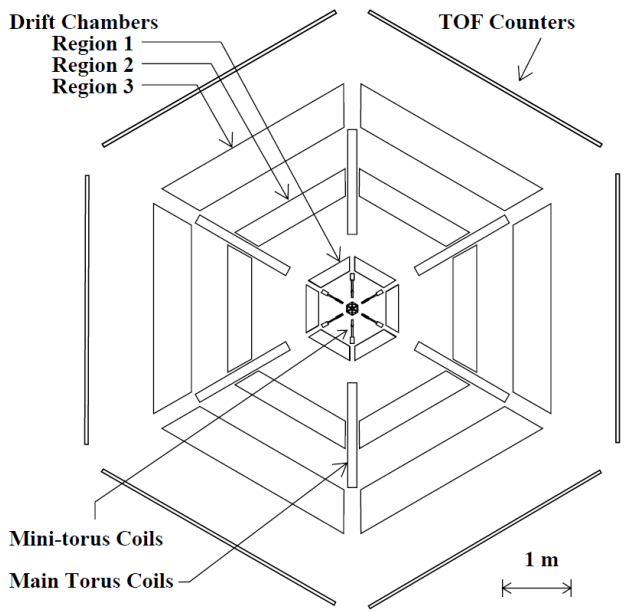

- Fixed target experiments.
- θ coverage between 8° to 142°.
- Complete ϕ coverage with six sectors in a hexagonally symmetric configuration.

B. A. Mecking et al., Nucl. Instrum. Methods Phys. Res., Sect. A 503, 513 (2003).

Outline

Basic Procedures & g12 Run Conditions

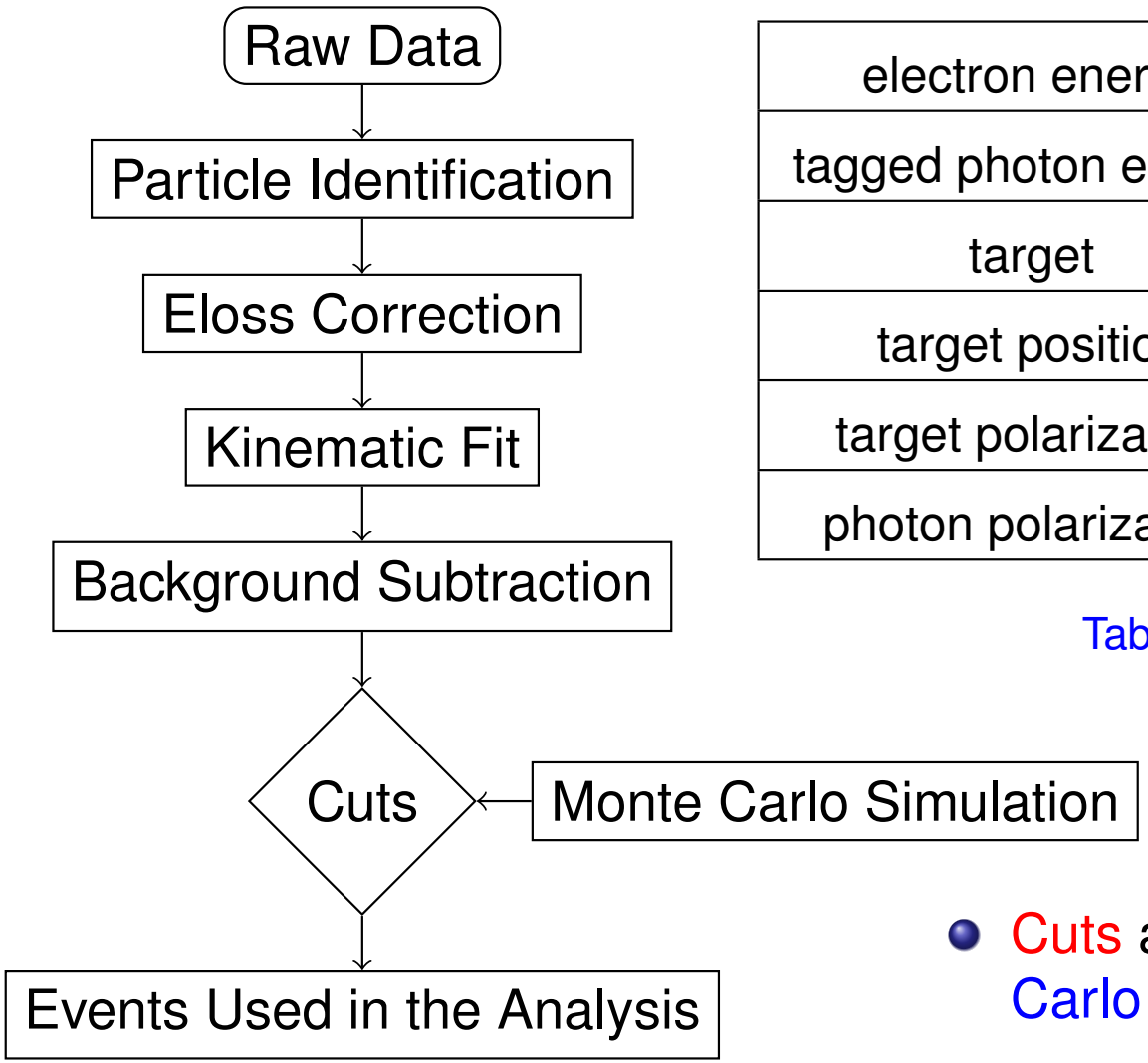

electron energy	5.715 GeV
tagged photon energy	1.1-5.45 GeV
target	liquid hydrogen
target position	$-110 < z < -70$ cm
target polarization	unpolarized
photon polarization	circular

Table: CLAS-g12 run conditions

- Cuts also applied to the Monte Carlo simulated events.

Kinematic Fit

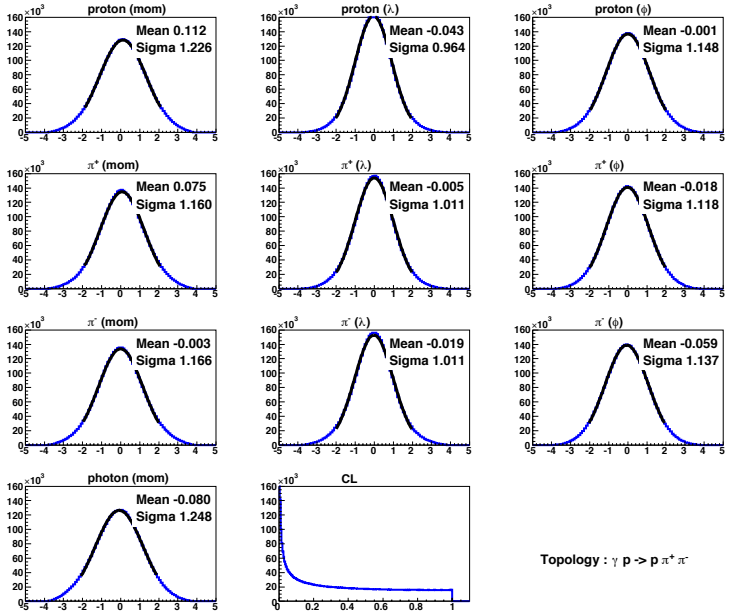

- Systematic effects would cause the center of the pull distribution shifted away from zero.
- Properly tuned covariance matrix makes the confidence level (CL) distribution flat toward CL=1.

- Enforcing energy and momentum conservation by varying 4-momenta of the final state particles.
- Important tool for monitoring and fixing errors in momentum measurements.

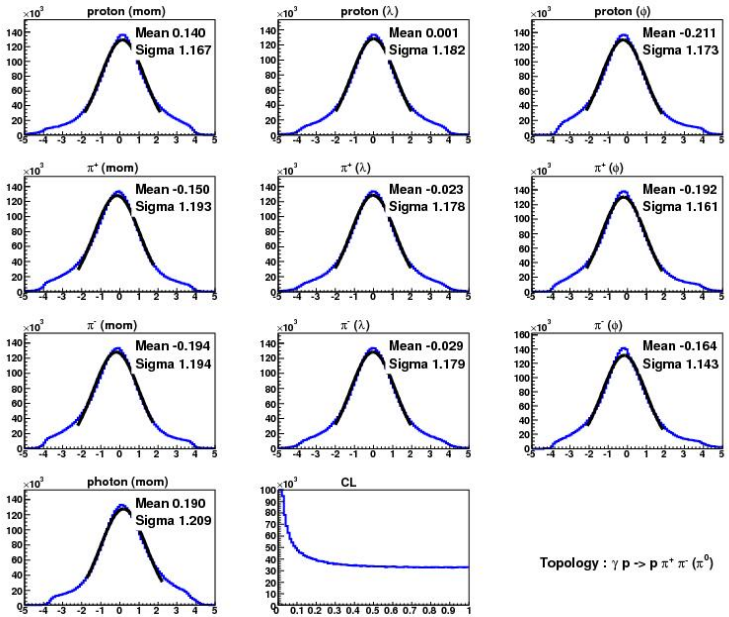

Background Subtraction Using the Q-factor Method

- Probability-based method: each event with an extracted Q-factor as its weight to be the signal.
- Measurements taken by summing over the Q-factors.

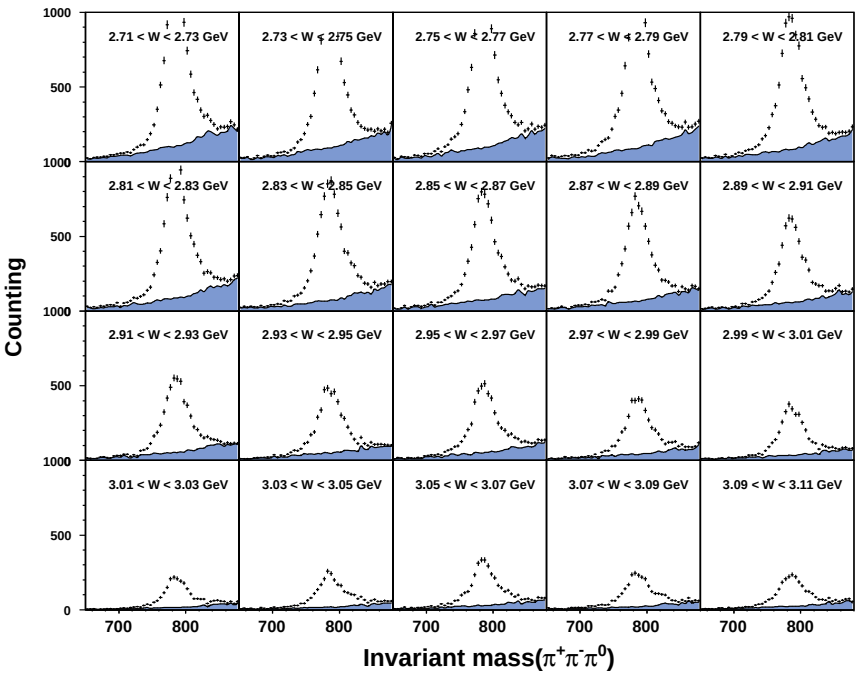

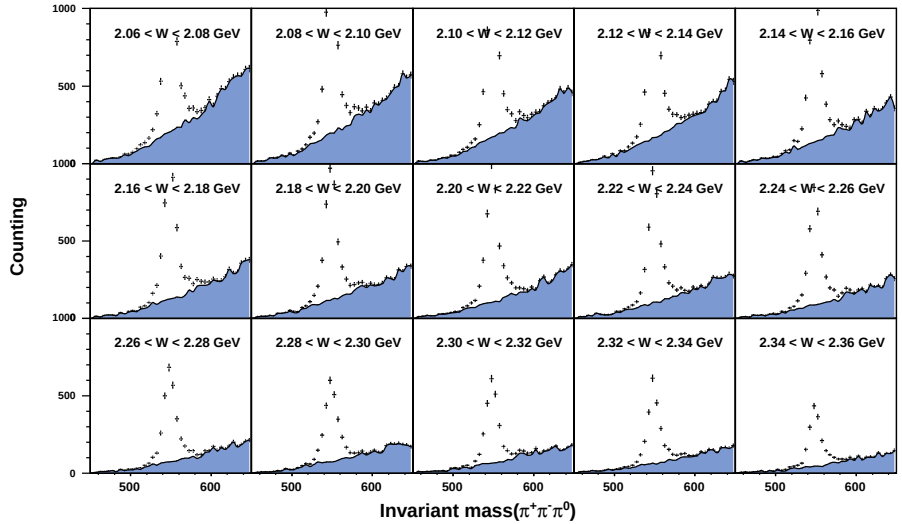

- Invariant mass distributions showing signal-background separation for $\gamma p \to p\eta$ (top) and $\gamma p \to p\omega$ (bottom).
- Data points with error bars are plotted with the full events while the distributions in blue are filled with a weight of $1 - Q$.

Coincidence Time Cut & $\Delta\beta$ Cut

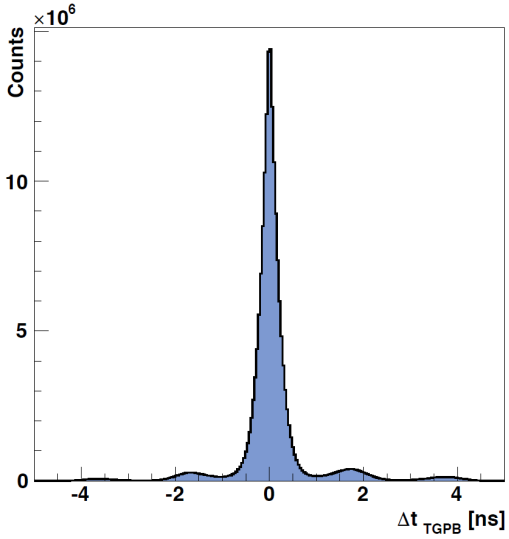

$$t_{event} = t_{ST} - \frac{d}{c\beta_m}$$
$$\Delta t_{TGPB} = t_{event} - t_\gamma$$

$$\beta_m = v/c$$
$$\beta_c = p/E$$
$$\Delta\beta = |\beta_m - \beta_c|$$

- Data events are considered only if $\Delta t_{TGPB} < 1$ ns.
- $\Delta\beta < 3\sigma$ is required for the proton or the π^+, to remove unseparated electrons.

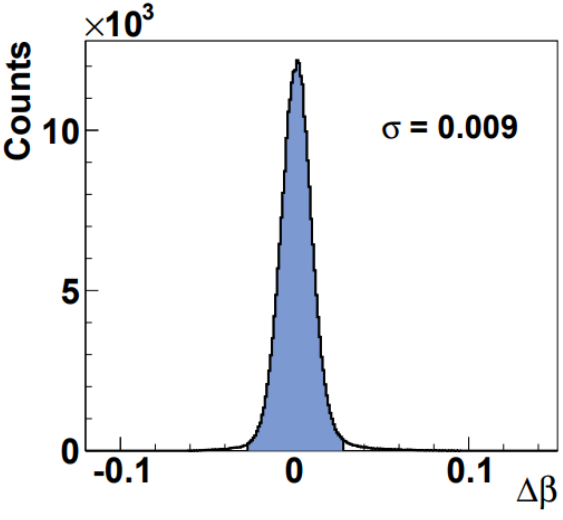

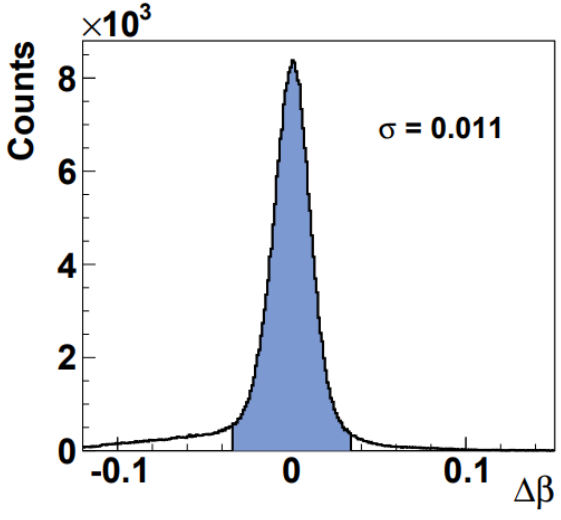

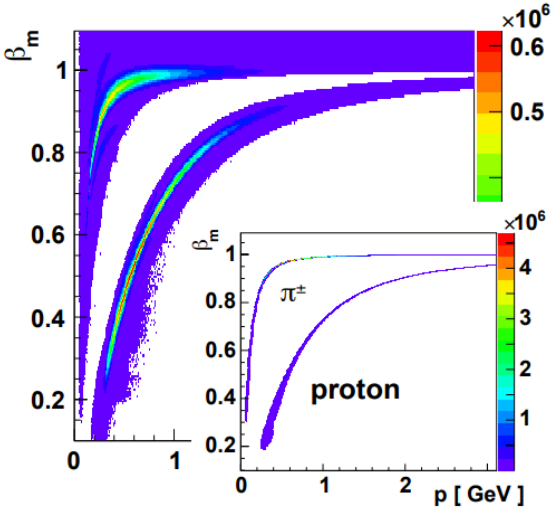

Trigger Cut & Trigger Efficiency Simulation

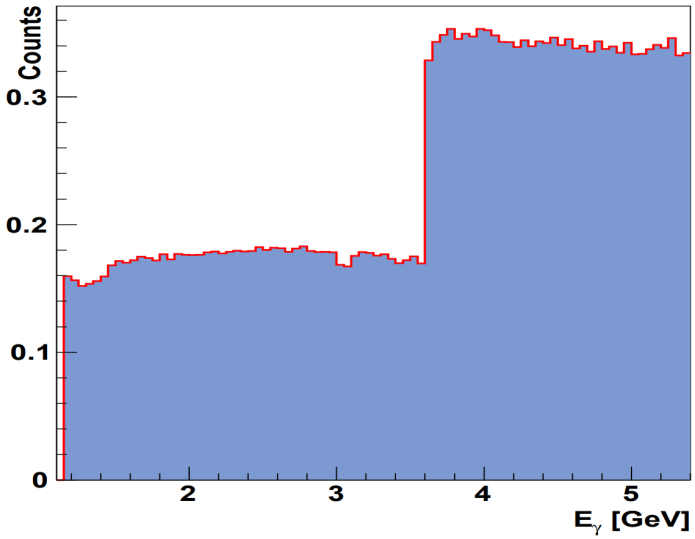

- Trigger efficiency mapped out for proton, π^+, and π^- over 6 sectors, 57 TOF paddles and the entire azimuthal angle.
- Trigger efficiency simulation only applied to the Monte Carlo events.

- Selected g12 runs with a mixture of 2-sector and 3-sector trigger conditions.
- Ratio distribution of 2-sector over 3-sector triggered events (left).
- Only 3-sector triggered data events kept for this analysis.

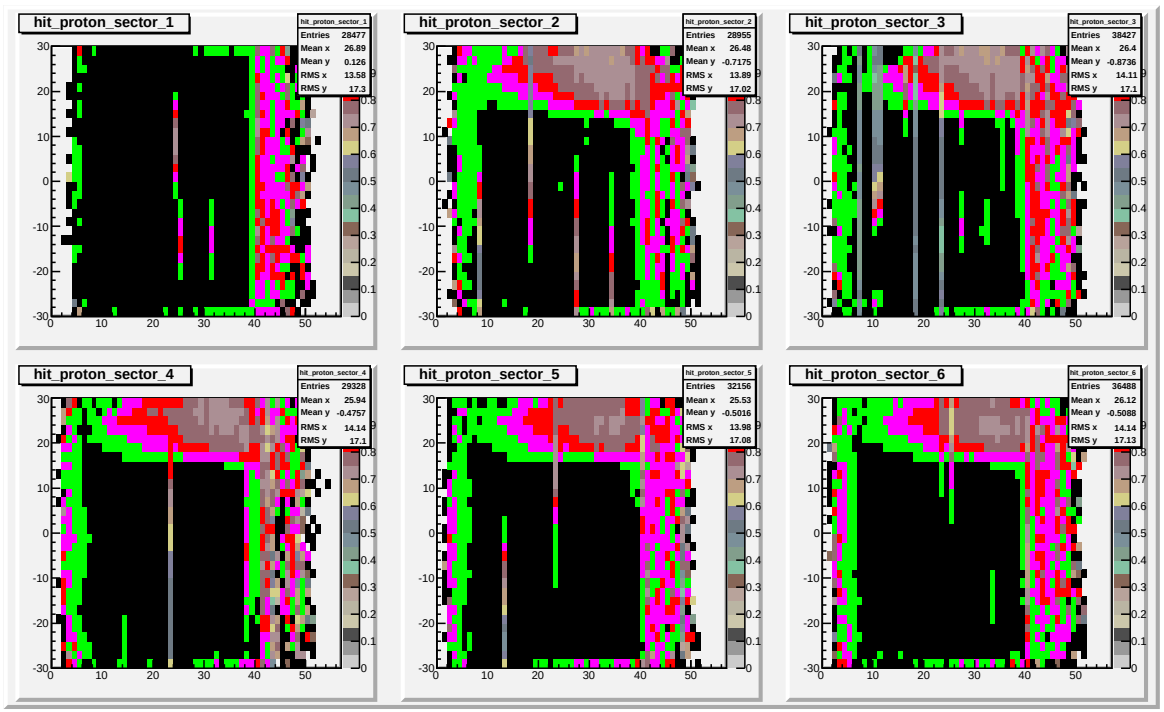

Z-Vertex Cut & Bad TOF Paddles

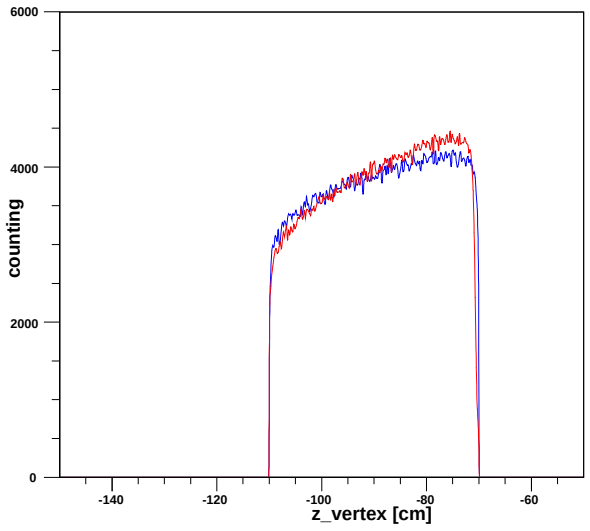

- Slight mismatch between the data and MC z-vertex distributions.
- Events from some TOF paddle removed for this analysis for being either inefficient or unstable during the run period.

Table: TOF paddles removed from this analysis.

Sector Number	TOF Paddle ID
1	6, 25, 26, 35, 40, 41, 50, 56
2	2, 8, 18, 25, 27, 34, 35, 41, 44, 50, 54, 56
3	1, 11, 18, 32, 35, 40, 41, 56
4	8, 19, 41, 48
5	48
6	1, 5, 24, 33, 56

Summary of the Cuts Applied

	Data	Monte Carlo
Confidence Level Cut	1%	
Coincidence Time Cut	$\Delta t_{\mathrm{TGPB}} < 1$ ns	
$\Delta\beta$ Cut	3σ	
Vertex Cut	$-110 < z < -72$ cm	
Forward π^0 Cut	$\cos\theta_{\pi^0}$<0.99	
Fiducial Cut	yes	
Trigger Cut	yes	
Trigger Efficiency Simulation	no	yes
Bad Paddle Knock Out	yes	

Table: Summary of the cuts that have been applied to this analysis.

Outline

$\gamma p \to p\eta$ Differential Cross Sections

Experimental form of the differential cross section:

$$\frac{d\sigma}{d\Omega} = \frac{N}{A}\frac{1}{N_\gamma \rho_{target}}\frac{1}{\Delta\Omega}\frac{1}{\mathrm{BR}},$$

N_γ: number of incident photons
ρ_{target}: area density of the target
$\Delta\Omega$: solid angle interval
BR: branching ratio

- $\gamma p \to p\eta$ differential cross sections measured in the dominant decay channel $\eta \to \pi^+\pi^-\pi^0$.
- Comparison with previous measurements as well as the η-MAID2018 solution and the BnGa2019 model.

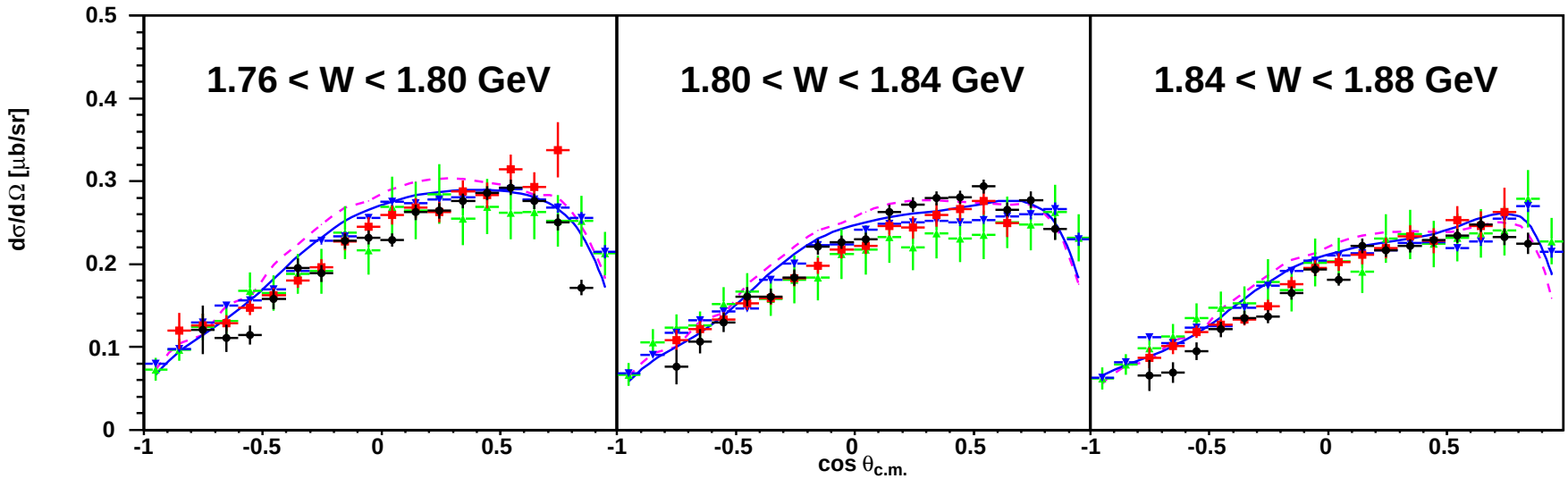

Published result: Phys. Rev. C 102, 065203 (2020).

$\gamma p \to p\eta$ Differential Cross Sections

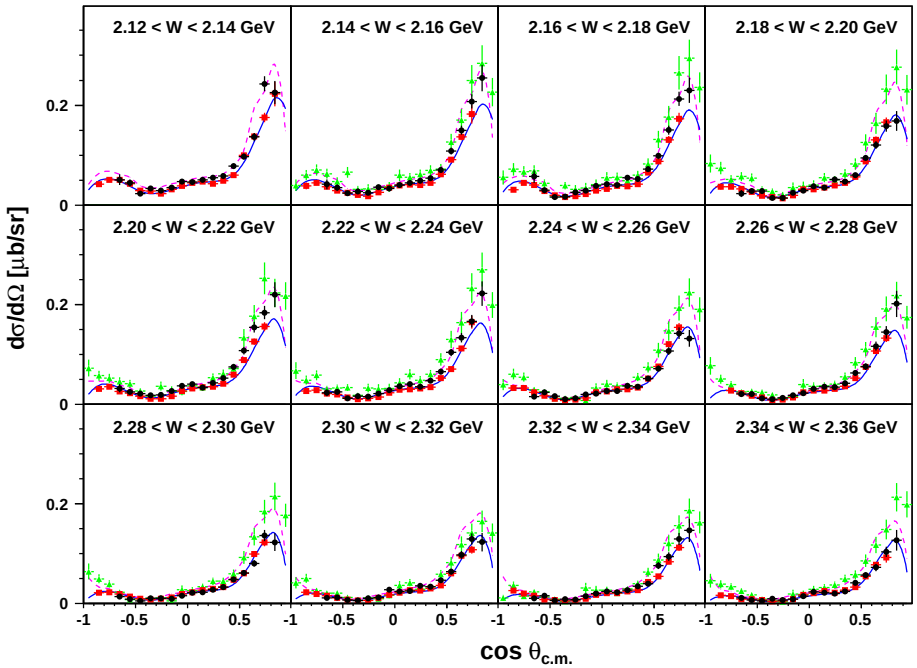

- The data confirms the dominance of the $1/2^-$ partial wave in both models.
- $N(1900)3/2^+$ resonance plays a significantly more important role in BnGa2019 than in η−MAID2018.
- Further identification of the resonance contributions also needs measuring polarization observables.

- Reasonable agreement in comparison with the SPring-8/LEPS measurement in Vs. W representation.
- A bump structure observed around $W \in [2.0,2.2]$ GeV (right picture).

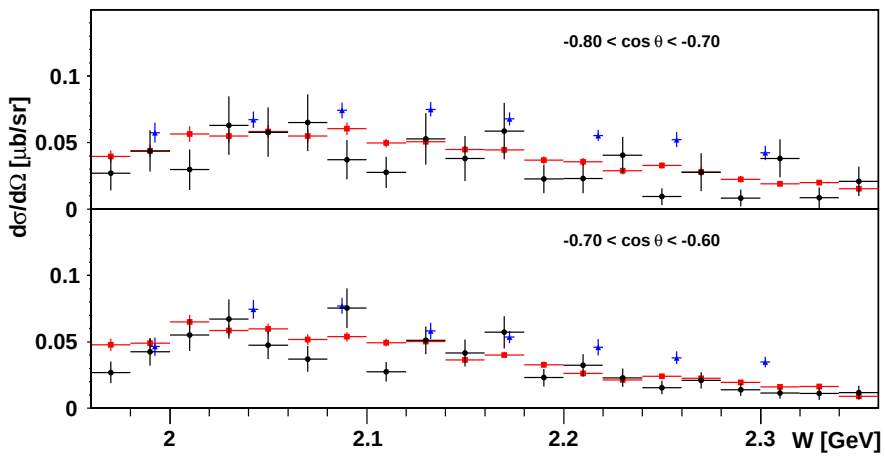

Published result: Phys. Rev. C 102, 065203 (2020).

$\gamma p \to p\eta$ Differential Cross Sections

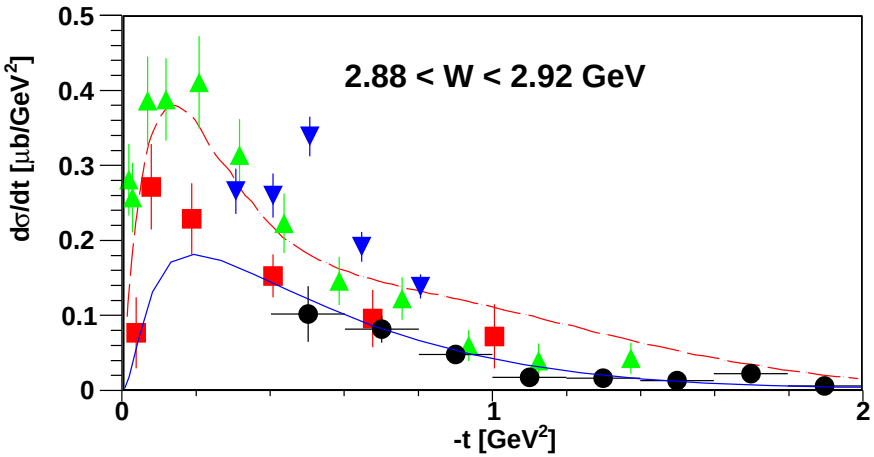

- $d\sigma/dt$ compared with MIT, Cornell, DESY, and NINA measurements, and η−MAID2018 and JPAC models.
- Production at $t = 0$ GeV^2 prohibited by angular momentum conservation.

- JPAC model: pure Regge model describing the process at low momentum transfer region ($-t < 1.0$ GeV^2).
- Our data are not in favor of inclusion of the 2^{--} tensor exchange, which would even scale up the cross section.

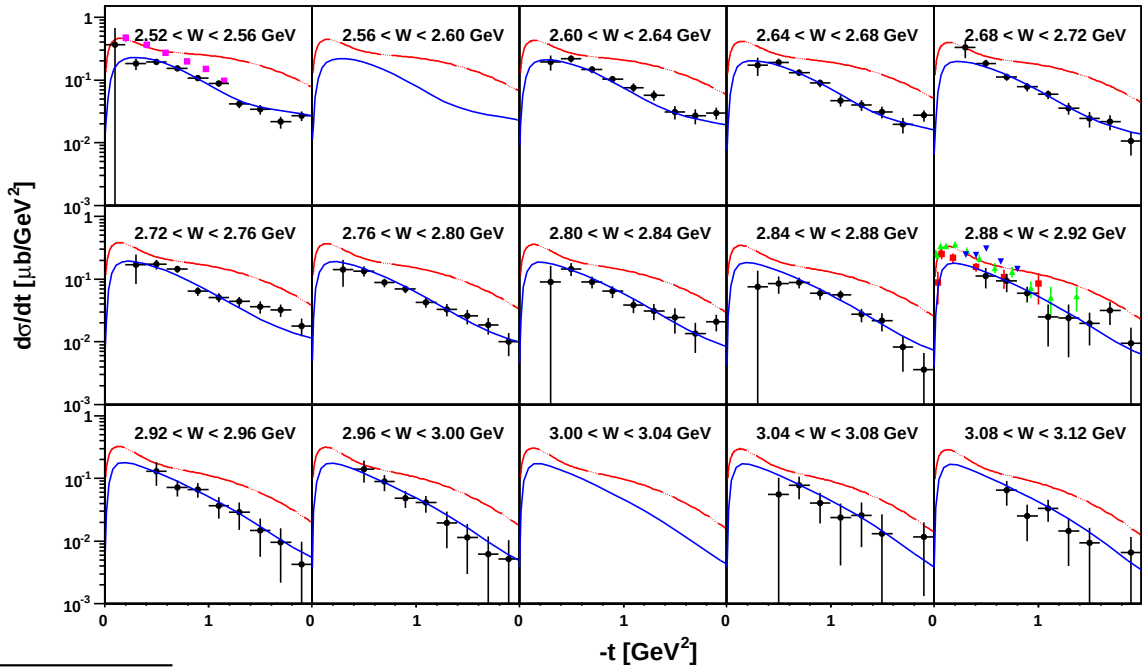

Published result: Phys. Rev. C 102, 065203 (2020).

$\gamma p \rightarrow p\omega$ Differential Cross Sections

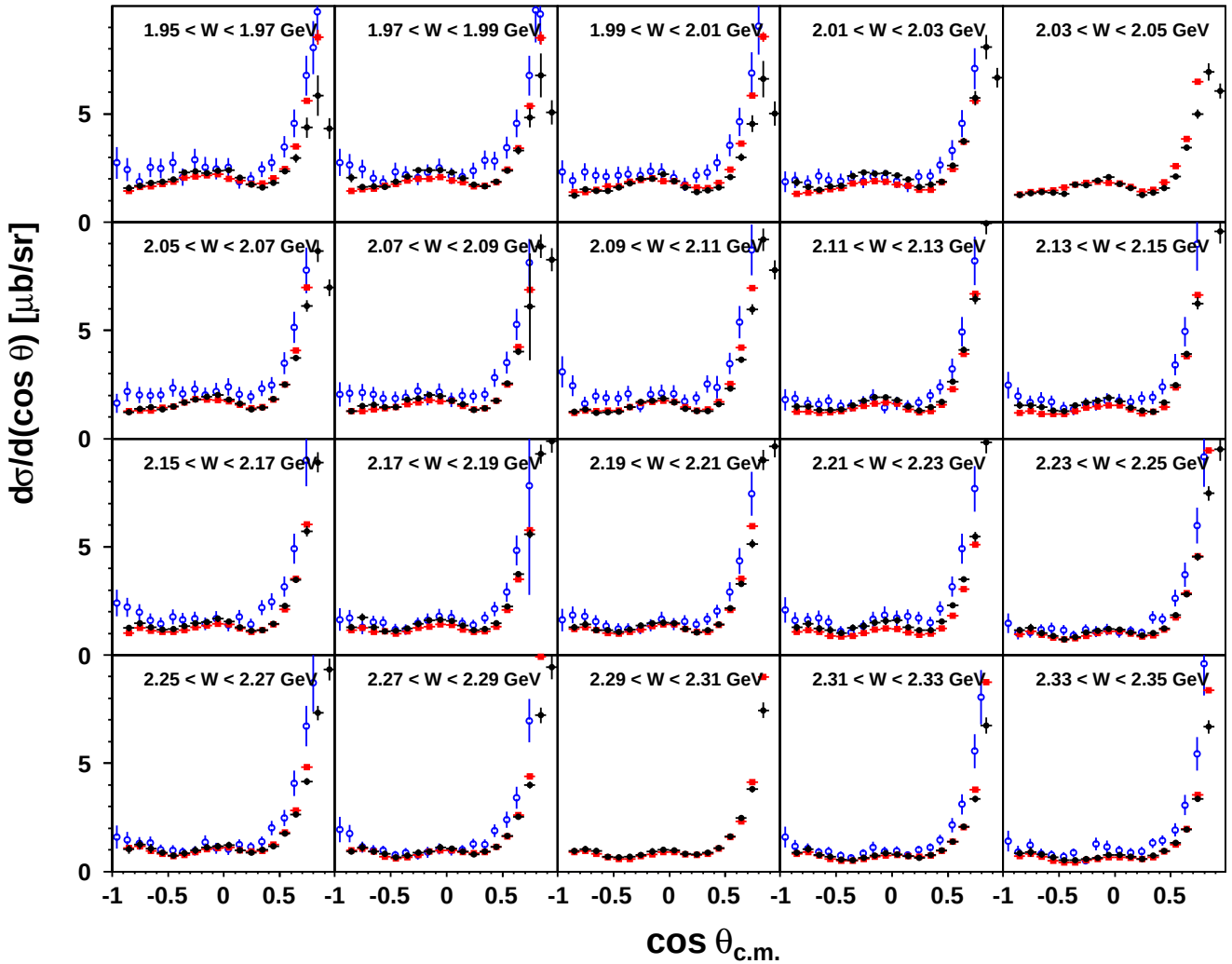

$\gamma p \rightarrow p\omega$ Differential Cross Sections

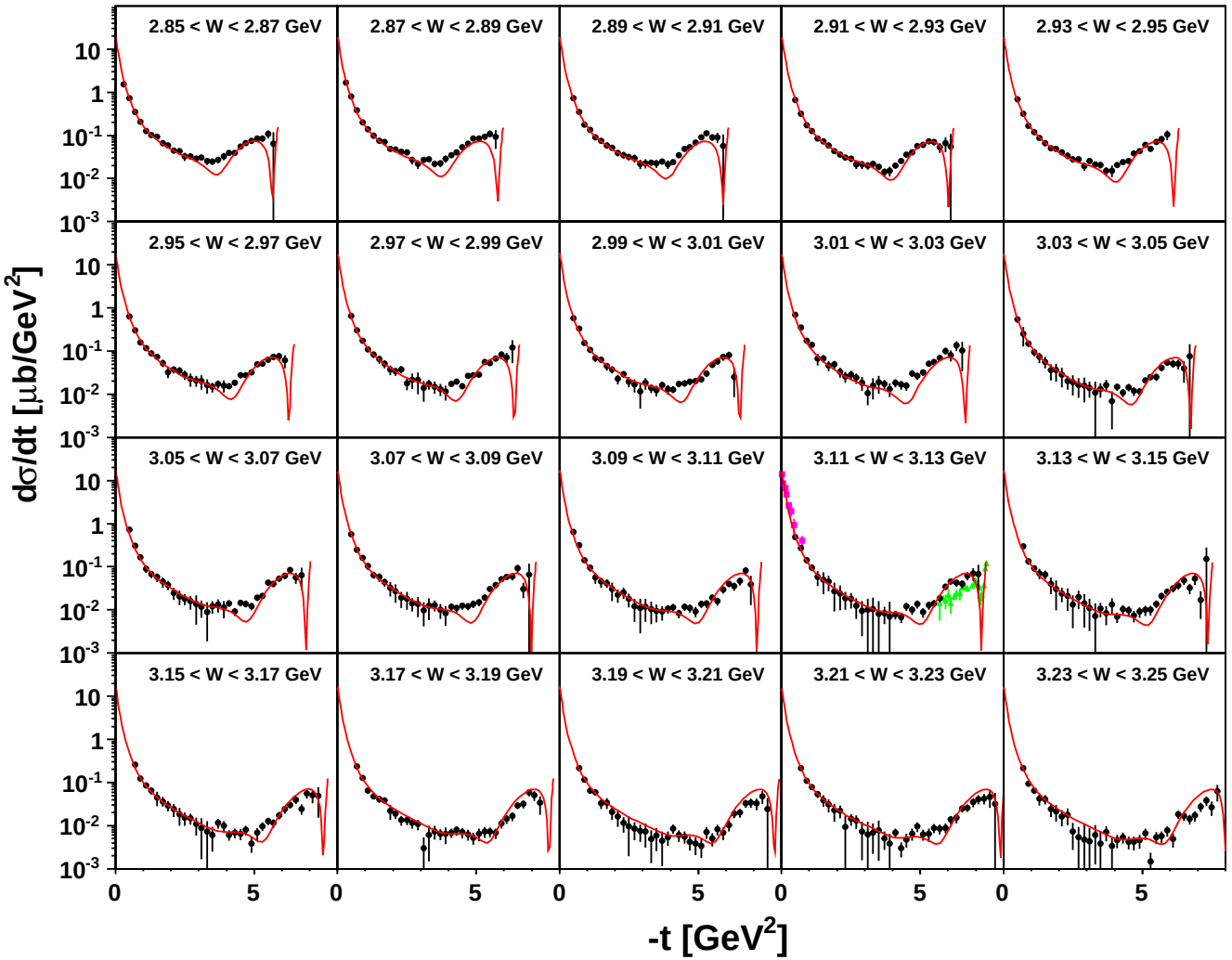

$\gamma p \rightarrow p\omega$ Differential Cross Sections

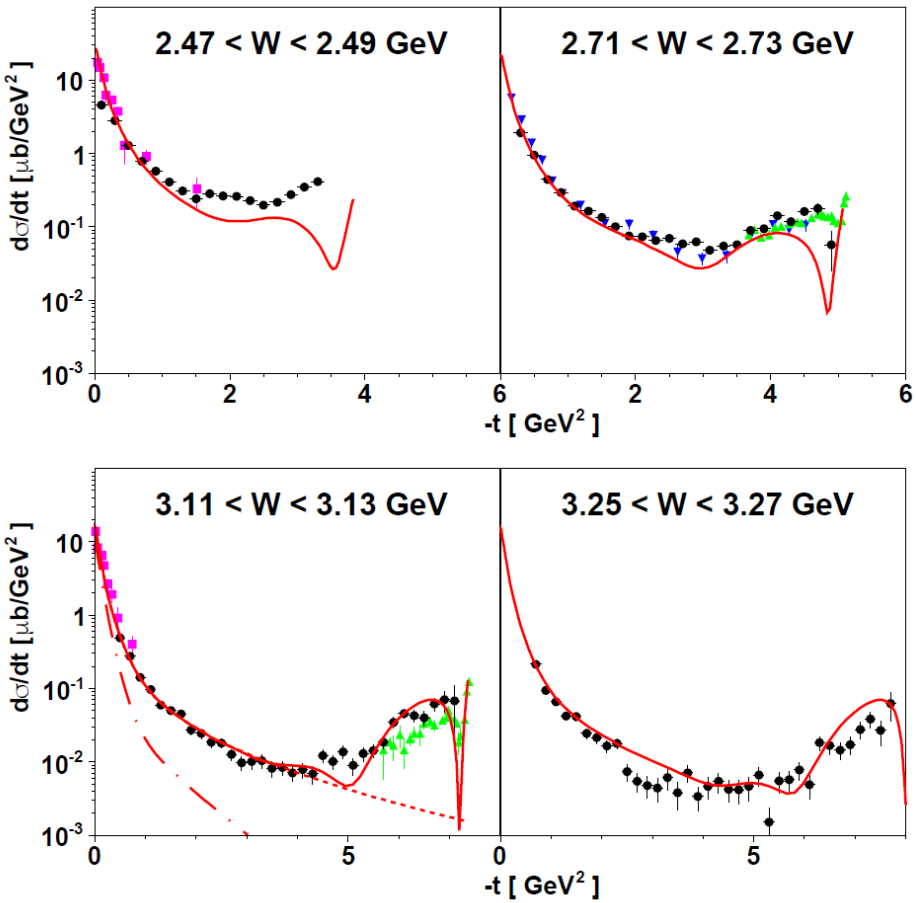

- Typical exponential behaviour due to Pomeron and Reggeon exchange observed at low momentum transfer, properly described by the model.
- The u-channel rise also observed at maximum momentum transfer.
- Dip predicted near maximum momentum transfer, which is not clearly seen in our data.

Results submitted to Phys. Rev. Lett.

Formulation

In the decay angular distribution, the unpolarized term and the circularly-polarized term are

$$W_0(\theta^*,\phi^*) = \frac{3}{4\pi}[\frac{1}{2}(1-\rho^0_{00}) + \frac{1}{2}(3\rho^0_{00}-1)cos^2\theta^* - \sqrt{2}Re(\rho^0_{10})sin2\theta^* cos\phi^* - \rho^0_{1-1}sin^2\theta^* cos2\phi^*], \tag{1}$$

$$W_3(\theta^*,\phi^*) = \frac{3}{4\pi}(\sqrt{2}Im(\rho^3_{10})sin2\theta^* sin\phi^* + Im(\rho^3_{1-1})sin^2\theta^* sin2\phi^*) \tag{2}$$

An event-based maximum likelihood fit was done to determine the SDMEs, with the likelihood function as

$$-\ln\mathcal{L} = \frac{\pi^3 C_\lambda (\sum_{i=1}^{n} Q_i)}{N_{rec}} \sum_{j=1}^{N_{rec}} (\lambda_j W_j) - \sum_{i=1}^{n} Q_i \ln W_i \tag{3}$$

$\gamma p \to p\omega$ SDMEs in the Adair Frame

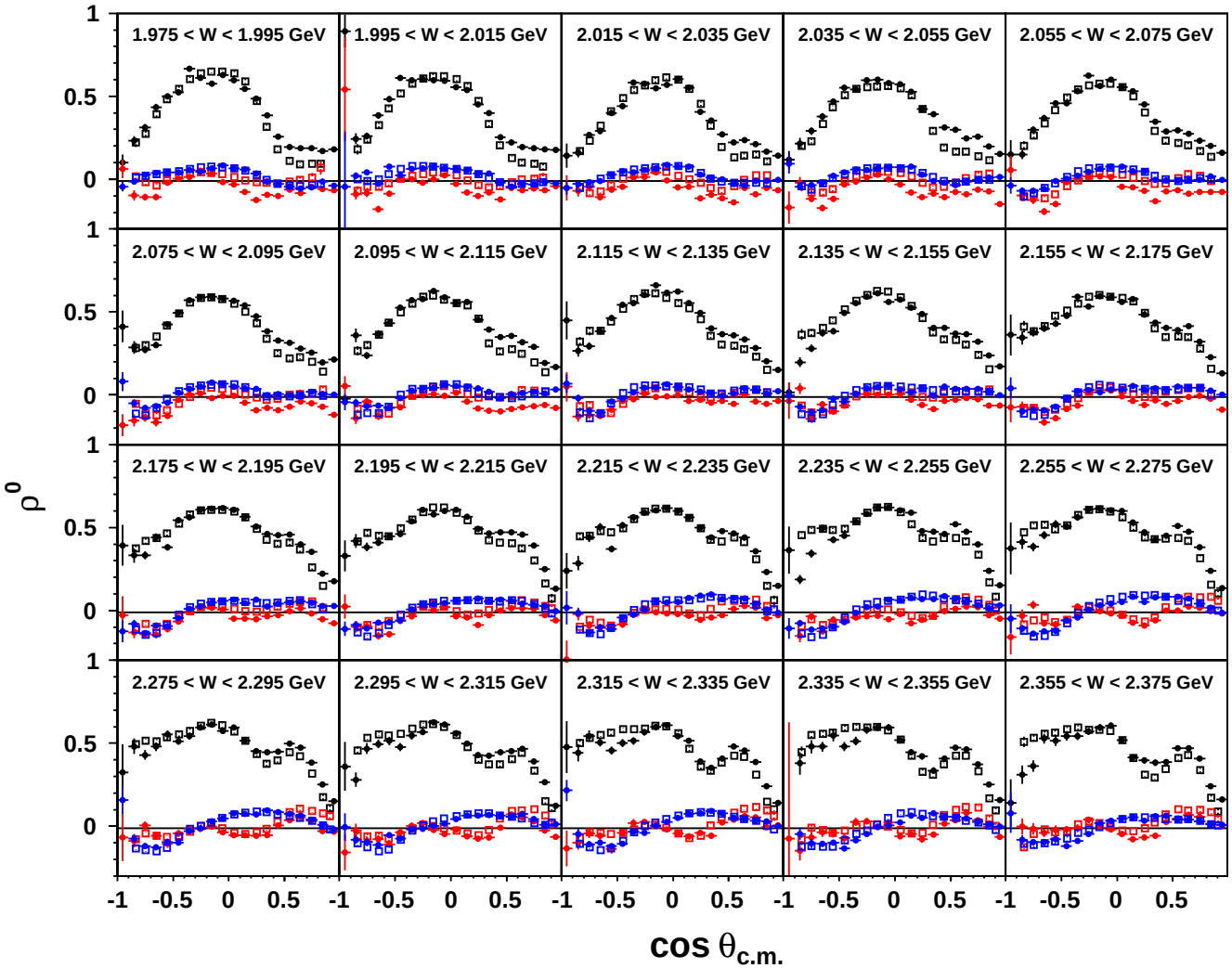

● CLAS-g12 □ CLAS-g11

Unpolarized SDMEs ρ^0 for $\gamma p \to p\omega$

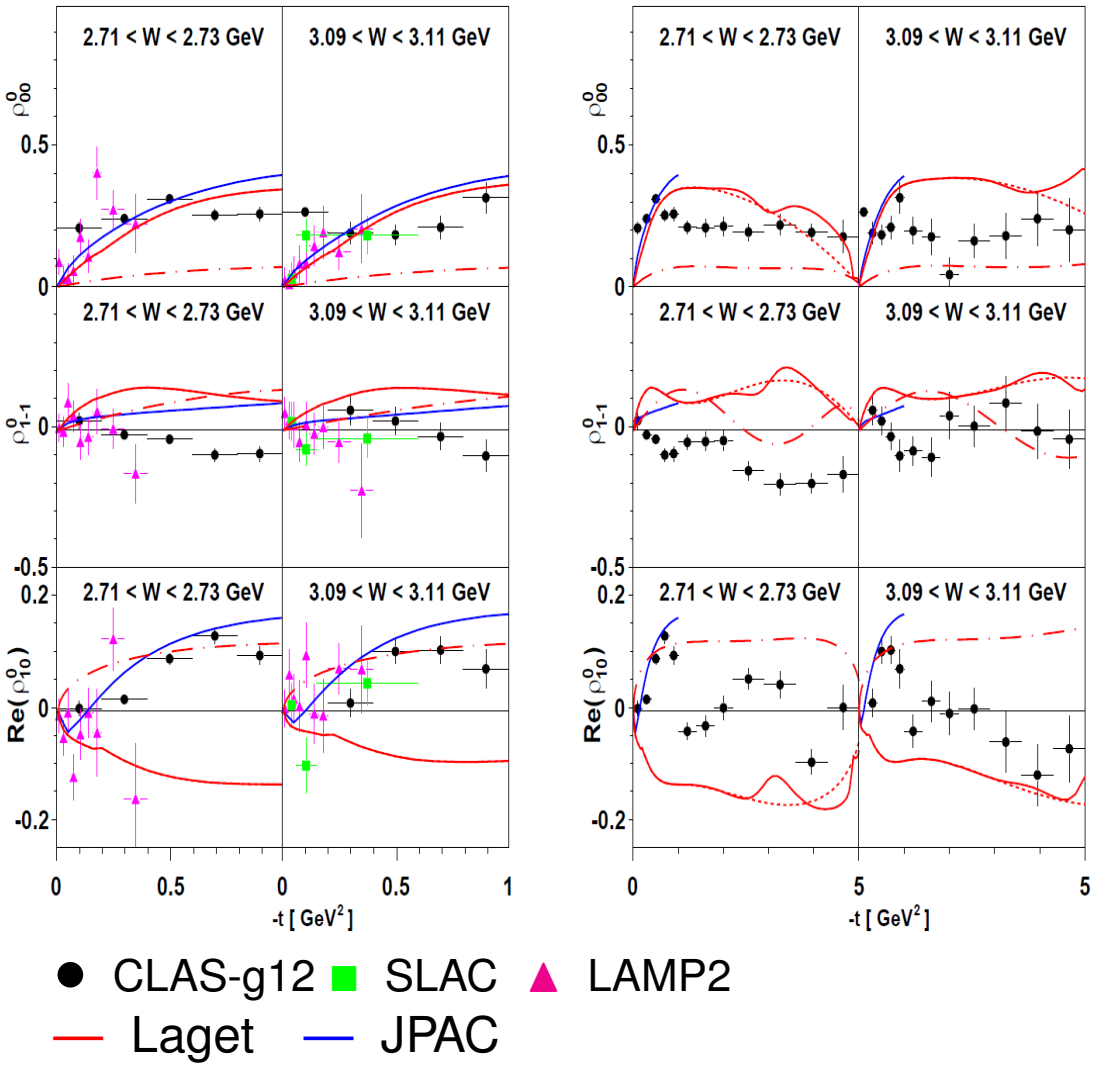

- The JPAC model properly describes ρ^0_{00} and Re(ρ^0_{10}) at small momentum transfer
- ρ^0_{1-1} has an opposite sign to the JPAC model prediction, indicating the new data are in favor of smaller contribution of the unnatureal-parity exchange than the model predicts.

Results submitted to Phys. Rev. Lett.

First Measurement of ρ^3 for $\gamma p \to p\omega$

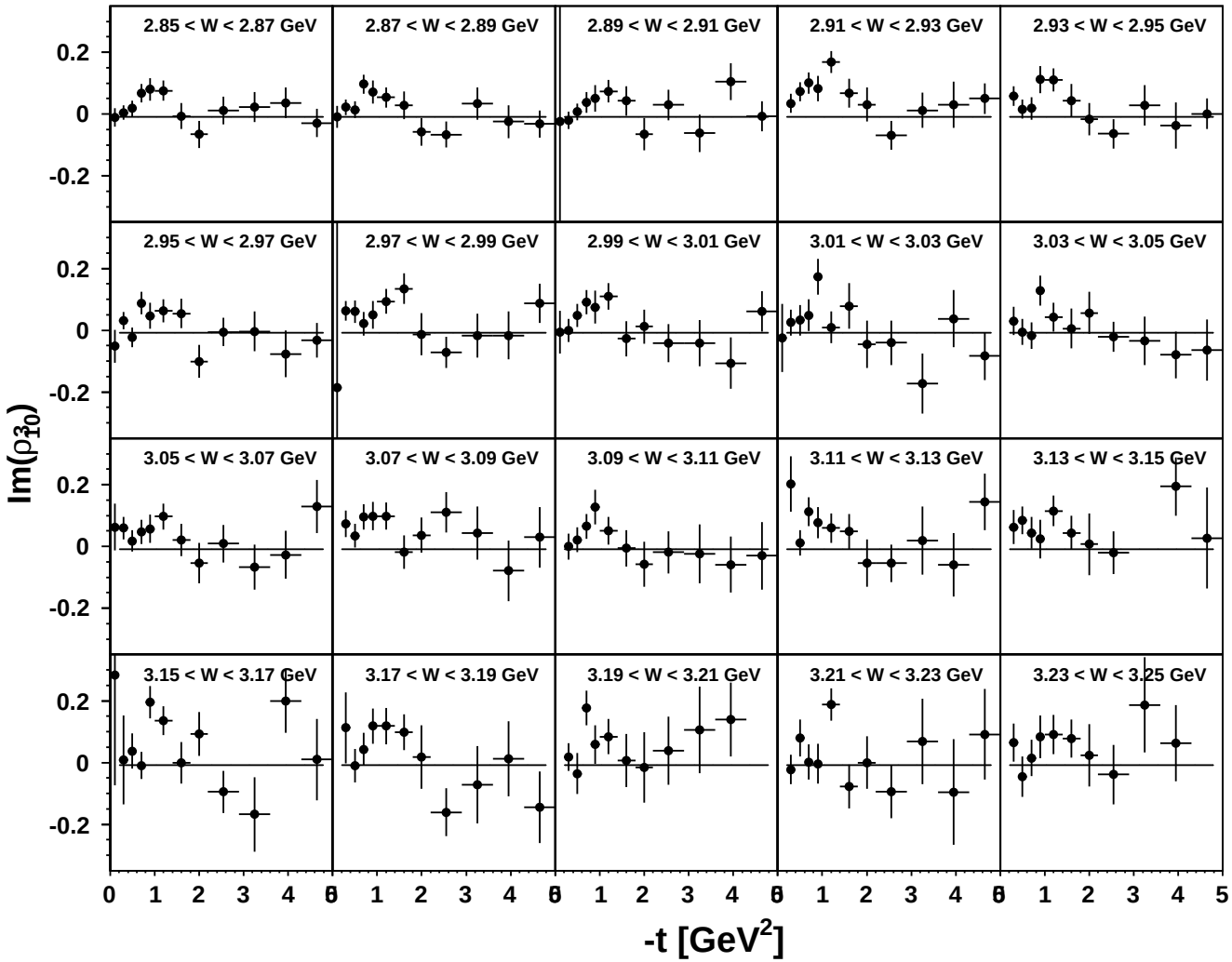

Results submitted to Phys. Rev. Lett.

First Measurement of ρ^3 for $\gamma p \to p\omega$

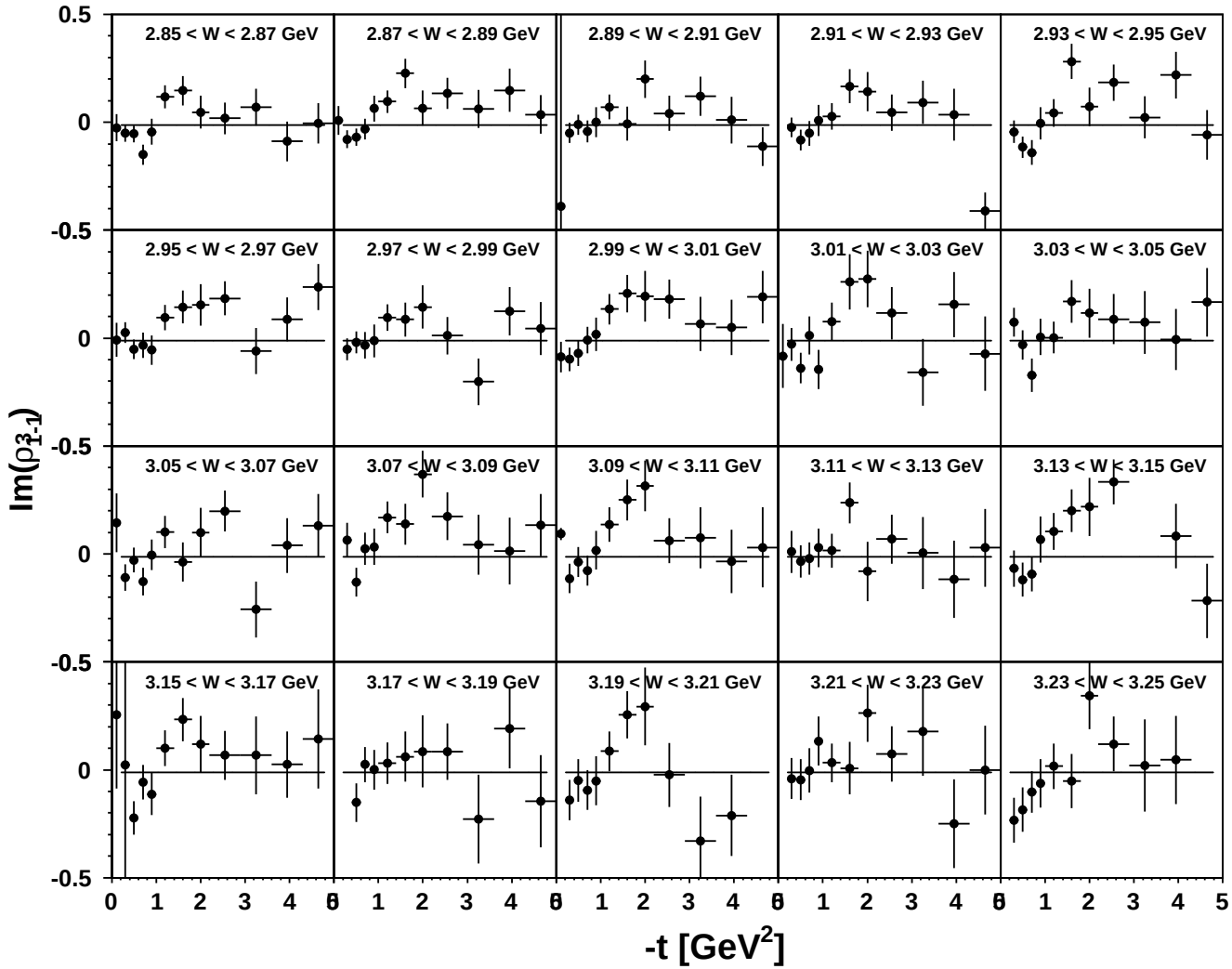

Results submitted to Phys. Rev. Lett.

Outline

Research Summary

- Our $\gamma p \to p\eta$ and $\gamma p \to p\omega$ differential cross section measurements extend the energy region above the resonance regime to $E_\gamma \approx 5$ GeV with relatively high precision compared with previous measurements. The new data could potentially be used for revealing $t-$ channel photoproduction mechanisms of pseudoscalar and vector mesons.
- The circularly polarized SDMEs ρ^3 for $\gamma p \to p\omega$ have been first measured, as well as the unpolarized SDMEs ρ^0 at large momentum transfer region $-t > 0.6$ GeV^2.
- The behavior of ρ^0_{00} and Re(ρ^0_{10}) is consistent with the model predictions, whereas ρ^0_{1-1} goes to the opposite sign direction relative to the models, indicating the new data are in favor of smaller contribution of the unnatureal-parity exchange than the model predicts.